Temperature dependence of photoluminescence in porous silicon and its interpretation using the porous-cluster model

N. Ookubo
Fundamental Research Laboratories, NEC Corporation, 4-1-1 Miyazaki, Miyamae-ku, Kawasaki, Kanagawa 216, Japan

S. Sawada
Department of Electrical and Electronics Engineering, Kagoshima University, 1-21-40 Korimoto, Kagoshima 890, Japan

(Received 3 November 1994; revised manuscript received 9 February 1995)

Photoluminescence (PL) of porous silicon in the redband is studied at temperatures from 15 to 293 K. With increasing temperature, the PL spectrum peak redshifts and the width narrows, while the PL intensity increases until ~70 K and then decreases slightly. At 293 K, the PL at higher emission energy decays faster with a broader rate distribution. The PL decay gets slower upon cooling, and becomes independent of emission energy below ~70 K. These results are qualitatively interpreted using a porous-cluster model that assumes random vacancy sites in a Si lattice. The low-temperature PL can be explained by carrier recombination through localized states which are distributed in energy, and dimensionally disordered. The changes in the PL with temperature, on the other hand, are understood by thermal activation of recombination processes, including hopping of carriers among distributed localized states.

I. INTRODUCTION

As possible mechanisms of redband photoluminescence (PL) from porous silicon, structural and optical studies have suggested excitonic recombination processes in nanometer-size crystals[1–7] and/or recombination through localized states on the surfaces of silicon nanocrystallites.[8–11] For example, a statement in favor of nanocrystallites has been put forward based on x-ray absorption data,[7] while surface properties rather than bulk ones have been insisted upon according to the fact that the PL persists even at high pressure where silicon crystal transforms to β-tin metallic phase.[11] Electron microscopy data have demonstrated on the one hand, the existence of silicon nanocrystallites[1–3] embedded in amorphous material, and, on the other, a microporous layer[12] with nanometer-size pores. Meanwhile, visible luminescence has been attributed to an effect of amorphous materials alone,[13–15] such as *a*-Si:H. Chemical substances such as SiH_x (Ref. 16) are less plausible since the samples almost passivated with oxygen show similar PL properties to those passivated with hydrogen.[17] Siloxene[18,19] has also been proposed, but an absence of the first neighbor Si-O bonds in x-ray absorption casts doubt on such a proposal.[20]

Changes in the PL emission band, i.e., green to red, and in the PL spectrum width have been reported for various samples, suggesting the light-emitting objects are distributed differently in different samples. This implies that the PL spectrum is inhomogeneously broadened, in accordance with the observation that the spectrum width is weakly dependent on temperature.[4,21] Upon cooling down from room temperature, the PL intensity is known to increase,[22–25] while the changes in the spectrum peak and width with temperature have been reported to be sample dependent.[21,23] Under resonant excitation at low temperature,[4–6] the PL spectrum is reported to have no resonant component but a structure presumably due to phonon satellites.

The PL decay has been observed at different time scales, e.g., picosecond to nanosecond[26] and submicrosecond to 10-millisecond[5,10,27–32] regimes. The fast decay becomes sizable only when an intense excitation is used.[26] The slow part shows nonexponential PL decay,[5,10,27–32] which has been well described by a stretched exponential,[10,30–32]

$$I = I_0 \exp[-(t/\tau)^\beta] , \tag{1}$$

where τ is a PL lifetime and β is an exponent describing the distribution of PL decay rates. The nonexponential profile has been observed to be persistent even for the narrow detection bandwidth, implying a distribution in recombination rates for the same emission energy. Equation (1), on the other hand, is the function often met in dispersive transport processes in disordered materials.[33] Such processes of photogenerated carriers are plausible in porous silicon due to random structures produced by distributions in size and spatial distance of nanocrystallites, and/or random terminations of surface Si atoms on nanocrystallites. Recently, the porous-cluster model, which assumes a network of silicon clusters rather than isolated nanocrystallites, has succeeded in yielding the stretched-exponential PL decay.[34] It is modeled on the microporous layer[12] with nanometer-size vacancies in porous silicon, and the PL decay is deduced by an analysis of the carrier dynamics on inhomogeneously distributed localized states which are produced by an irregular distribution of atoms in a two-dimensional Si lattice.

The PL lifetime at room temperature has been known to decrease exponentially with emission energy.[25,27–32] This behavior has been ascribed to carrier tunneling through a surface SiO_2 layer to nonradiative paths, with

0163-1829/95/51(24)/17526(9)/$06.00 ©1995 The American Physical Society

the rate increasing with confinement (or emission) energy.[25] Also known is that the PL lifetime decreases as the number of electron-spin resonance (ESR) centers increases by thermal annealing.[28,30] Because of the close similarity to the Pb center,[35,36] the ESR centers have been conceived to be Si dangling bonds, which serve as the nonradiative paths. The increase in the PL lifetime by cooling the sample has thus been ascribed to the suppression of carrier transitions to nonradiative paths.[24,25] The PL lifetime dependence on temperature over a wide range, 7 to ~300 K, has otherwise been explained by variable range hopping of carriers[10,37] at the crystallite-SiO_2 interface,[10] although no explanation is given for the change in the PL lifetime with emission energy. Alternatively, the variation in the PL lifetime with temperature has been explained by the change in the relative population of carriers in triplet and singlet states, but without assuming nonradiative processes.[5,6] The reason for the distribution of the PL decay rates in these models, however, has not yet been sufficiently described.

In this paper, we present in Sec. III the results on PL spectra and decays of porous silicon at temperatures from 15 to 293 K, after Sec. II for experimental procedures. Then, a qualitative but unified understanding based on the porous-cluster model is given in Sec. IV, with a brief introduction to the model and carrier kinetics (Sec. IV A). The calculation is extended to the PL spectra and the PL decays under various conditions, including dominance of radiative processes (Secs. IV B and IV C). In Sec. IV D, we discuss dimensional disorder in the electronic structure of the model to explain the statistical effects, i.e., the PL lifetime and the rate distribution independence from emission energy.

II. EXPERIMENT

Porous silicon was prepared by anodizing a silicon substrate (B doped, ~10 Ω cm) in a HF solution ($HF:H_2O:C_2H_5OH=1:2:1$) with a current density of 13 mA/cm^2 for 0.4 h. The sample was rinsed in deionized water, dried under an N_2 gas flow, and stocked for one month in ambient conditions after thermal annealing at about 300 °C for 5 min under an N_2 gas flow. The last process yielded an oxidized porous silicon with an ir absorption band at 1100 cm^{-1} due to Si-O-Si vibration. As compared to the unannealed sample, the sample thus obtained showed excellent stabilities to laser illumination and to environments. Further, it exhibited the faster PL decay with a wider distribution of decay rates, similar to a previous report.[30] The thickness of the porous layer was about 8 μm and the porosity estimated by weight was about 65%.

The PL was excited by pulsed light from an N_2 gas laser. Its wavelength is 337 nm; a pulse frequency is 1~4 Hz; a pulse width is 30 ns; and a pulse energy is about 20 μJ. Its intensity is low enough (≤ 10 mW/cm^2) to give the slow PL process alone.[26] The sample was set in a holder cooled by a cryopump system. The PL decay was detected after passing the PL through a monochrometer (HR 320, Jobin-Ybon). The photocurrent signal from a photomultiplier (H957, Hamamatsu Photonics) was retrieved by accumulating digitized decay signals in a digitizer (PM 3320, Philips). The PL spectrum was measured under an excitation by a monochromatic light, and calibrated for dispersion efficiency of the monochrometer and cathode efficiency of the photomultiplier.

III. RESULTS

A. Luminescence spectrum

Figure 1 (bottom) shows the PL spectra under excitation at 3.873 eV for different temperatures. Dots represent experimental results and solid curves are calculated according to a Gaussian function,

$$I=(Q/\sqrt{2\pi}\sigma)\exp[-(E-E_p)^2/2\sigma^2], \tag{2}$$

where I is the emission intensity at energy E, Q is the emission intensity integrated over E, σ is the spectrum width, and E_p is the energy of the spectrum peak. Similar to a previous study,[31] the Gaussian function well describes the spectrum profile. With decreasing temperature, E_p shifts to the high-energy side (blueshift), σ broadens, and Q increases until about 70 K and then slightly decreases as shown in Fig. 1 (top).

B. Luminescence decay

The PL decays and fits to a stretched exponential [Eq. (1)] are shown in Figs. 2 and 3. At 293 K, the PL decay changes with emission energy E_{PL}. It is faster and more dispersive for larger E_{PL} (top of Fig. 2). The fits are satisfactory. The PL decays at a constant E_{PL} for different temperatures (bottom of Fig. 2) show that the decay gets

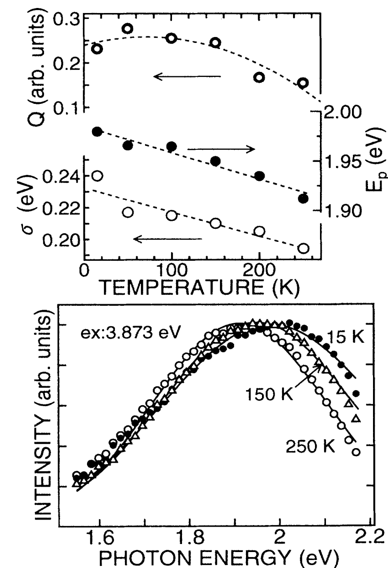

FIG. 1. Photoluminescence spectra taken at different temperatures (bottom). Dots represent experimental data and solid curves are fits to a Gaussian function [Eq. (2)]. Plots of fit parameters (top), Q (integrated PL intensity), E_p (spectrum peak), and σ (spectrum width) vs temperature.

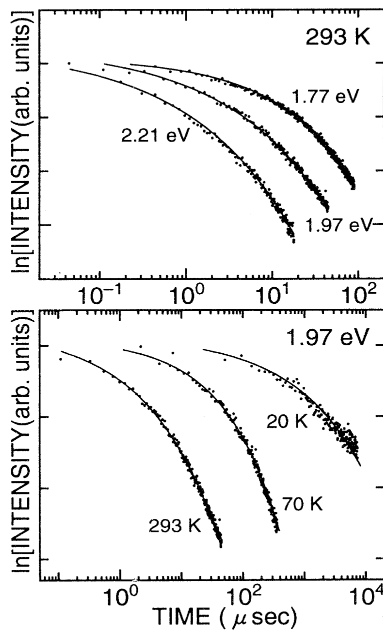

FIG. 2. Photoluminescence decay at representative emission energies at 293 K (top), and at 1.97 eV for different temperatures (bottom). Dots are experimental results and solid curves are fits to a stretched-exponential function [Eq. (1)]. The ordinate scale has an arbitrary origin for each curve.

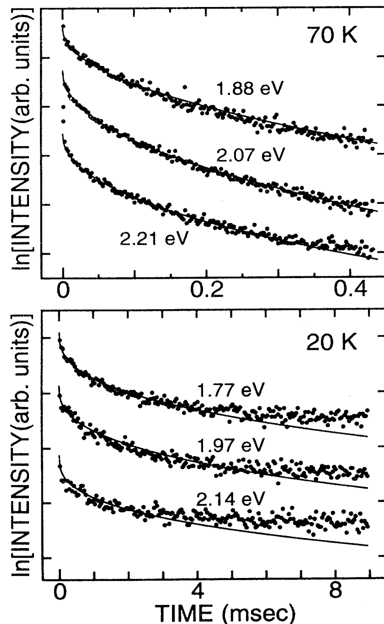

FIG. 3. Photoluminescence decay at low temperatures. Dots and solid curves have the same meaning as in Fig. 2. Note top and bottom figures have different time scales and in the bottom the fits are unsatisfactory for $t \gtrsim 4$ msec.

remarkably slower with decreasing temperature. Below ~ 70 K, the PL decay becomes independent of E_{PL} (see top of Fig. 3). Moreover, the fit becomes unsatisfactory. At 20 K, the fits obtained by weighting the initial PL decay data (bottom of Fig. 3) show that the stretched-exponential curve is below the experimental decay data at large t.

The values of the PL lifetime τ obtained by the stretched-exponential fits are shown in Fig. 4. At 293 K, τ has a value in the range $10^{-7}-10^{-5}$ sec and shows a steep exponential decrease with E_{PL}. Upon cooling, this decrease becomes gradual and mostly disappears below ~ 70 K. At 20 K, τ has a very large value (~ 2 msec). Note the continuous increase in τ by cooling while the integrated PL intensity Q increases until ~ 70 K and then slightly decreases (Fig. 1). The dashed lines on the plots of τ versus E_{PL} in Fig. 4 are the least-square fits to a function $\ln \tau \sim -E_{\mathrm{PL}}/E_T$. It appears that E_T is a linearly decreasing function of temperature (inset to Fig. 4). To show how τ at different E_{PL} changes with temperature T, $1/\tau$ is plotted against T^{-1} (lower left of Fig. 5) or $T^{-1/4}$ (upper right of Fig. 5) for representative values of E_{PL}. Apparently, $1/\tau$ is linear for $E_{\mathrm{PL}} = 1.65$ eV in the former plot and for 1.97 eV in the latter. The plot of $1/\tau$ versus $T^{-\zeta}$ at different E_{PL} thus appears to be linear for different value of ζ.

On the other hand, the distribution parameter β for various PL decays is shown in Fig. 6. Here, a smaller β means apparently a broader distribution of decay rates. In the top of Fig. 6, β at 20 K is small and almost unchanged with E_{PL}. With increasing temperature, β becomes a slightly decreasing function of E_{PL} and, at 293 K, its change with E_{PL} is steep. As temperature changes (bottom of Fig. 6), β appears as an increasing function of temperature for small values of E_{PL}, e.g., 1.65 eV, while β for large values of E_{PL}, e.g., 2.29 eV, increases with temperature until ~ 70 K and then decreases.

The above results are summarized briefly: Upon temperature decrease, the PL spectrum peak blueshifts and

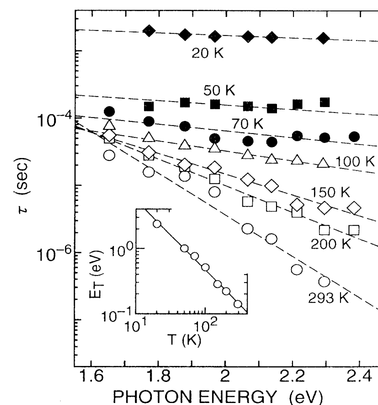

FIG. 4. Photoluminescence lifetime τ for the decay at various emission energies at temperatures from 20 to 293 K. Dashed lines are least-square fits using a function $\ln\tau \sim -E_{\mathrm{PL}}/E_T$ where E_T is plotted in the inset.

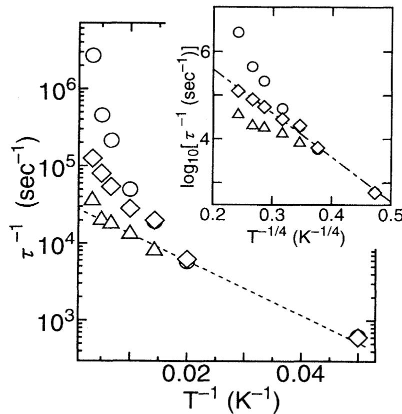

FIG. 5. Plots of τ^{-1} vs T^{-1} for different emission energies: 2.29 eV (○), 1.97 eV (◇), and 1.65 eV (△). The dashed line is drawn using a value of 9 meV for the activation energy W' (see Sec. IV B). In the inset the same data are plotted vs $T^{-1/4}$ and the dashed-dot line is a fit to the data of 1.97 eV.

its width broadens. While the integrated PL intensity increases and shows a slight decrease below about 70 K, the PL lifetime increases throughout the temperature range examined. At 20 K, both the long PL lifetime and the broad distribution in the decay rates are almost unchanged with E_{PL}. Above ~70 K, the PL lifetime is an exponentially decreasing function of E_{PL}, which is steeper at higher temperature, and the distribution in the decay rates is broader for larger E_{PL}.

IV. DISCUSSION

Radiatively recombining electron-hole pairs in porous silicon have been assumed to be spatially separated[22,30] or spatially confined.[1–6] In the former, carriers (electrons and/or holes) are trapped in localized states, move by hopping, and/or recombine through tunneling. Carriers are often assumed to reside in localized states at the crystallite-SiO_2 interface[8–10] because ESR centers, which critically affect the PL,[28,30] are conceived to be Pb centers at the crystallite-SiO_2 interface.[35,36] Further, the PL spectrum has been observed to be insensitive to the average size of the silicon nanocrystallites covered by a SiO_2 layer,[10] suggesting surface-localized rather than confined states are plausible. The change of the PL lifetime with temperature has thus been ascribed to two-dimensional variable range hopping,[10] which predicts $1/\tau$ proportional to $T^{-1/3}$. This description, however, is insufficient since $1/\tau$ for different E_{PL} appears to be proportional to $T^{-\zeta}$ for different ζ (Fig. 5). The linearity for $\zeta=\frac{1}{4}$ may give an occasional possibility of variable range hopping in *three* dimensions.[37]

Meanwhile, the concept of spatially separated electron-hole pairs has often been applied to a variety of PL characteristics observed in amorphous semiconductors.[38] Carriers separated by R assume a recombination rate proportional to $\exp(-2R/R_B)$ for $R \gg R_B$. Here, R_B is the size of the wave function, assumed to fall off isotropically as $\exp(-R/R_B)$. In the simplest case, R_B is the size of the larger of the two (electron and hole) wave functions. Since R_B is smaller for deeper tail states which yield lower emission energies,[38–40] this expression of the rate implies for randomly distributed R that the PL lifetime decreases as the emission energy increases, as actually observed in *a*-Si:H at low temperature.[38] Porous silicon, however, behaves so only at temperature above ~70 K and the behavior is more pronounced at higher temperature (see Fig. 4). As another example, *a*-Si:O:H alloy has been known to show an intense visible PL even at room temperature,[41] similar to porous silicon. Its PL lifetime is mostly independent of emission energy, which is understood in the way that the emission energy is decoupled from R_B by the Coulomb interaction between recombining electron-hole pairs.[41] This dependence in *a*-Si:O:H, however, appears at room temperature, while porous silicon exhibits such dependence only at low temperature. The PL mechanism of these amorphous materials is thus insufficient to model directly the PL in porous silicon.

When the electron-hole pairs are assumed to be confined in nanocrystallites,[1–7] various sizes of nanocrystallites will produce different confinement energies and thus yield a broad PL band. If the confined state is further assumed to split into singlet and triplet states[5,6] with an exchange energy enhanced by confinement,[42] carriers will tend upon a temperature decrease to populate triplet states with longer recombination times, thus resulting in the PL-lifetime increase. This model may be plausible if an additional assumption is acceptable, namely, that nanocrystallites having *the same size but a distribution in shapes*[5,6,24] will yield nonexponential PL decay at a single emission energy. However, surface properties rather than bulk ones have been put forward as the origin of the PL since porous-silicon PL survives even under high pres-

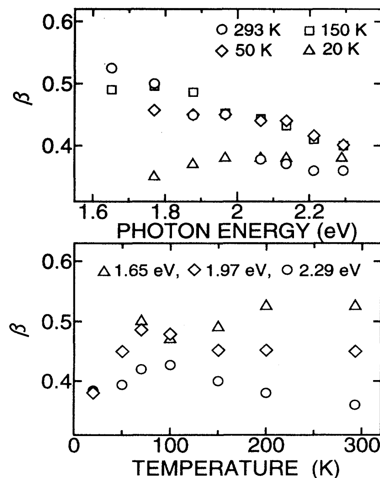

FIG. 6. Distribution parameter β for various photoluminescence decays plotted vs emission energy (top) and temperature (bottom), respectively.

sure[11] ($\gg 13$ GPa) when silicon crystal is in the β-tin metallic phase which has *no* band gap. In addition, the negative pressure coefficient for the PL spectrum shift also makes it difficult to attribute the origin of the PL straightforwardly to simple quantum confinement effects.[11,43]

A. Porous cluster model and luminescence kinetics

To explain the observed results, we apply the porous-cluster model which is known to yield PL decays describable by a stretched exponential.[34] Recall that the irregular structures in porous silicon[12,34,44] contain many voids which are distributed mostly in two pore sizes; *macropores* larger than ~ 50 nm wide covered with a *microporous* layer having pores smaller than 2 nm wide.[12] While macropores mainly contribute to the porosity, the microporous layer represents a network of atomic clusters rather than an ensemble of isolated nanocrystallies. Electronic levels in this layer may be localized, spread in energy, and form bands of localized states, thus producing luminescence due to spatially separated carriers. The porous-cluster model represents these features by assuming random vacancies of site atoms in a two-dimensional Si lattice.[34] By using a tight-binding-model calculation,[45] it is not necessary to assume carriers to be distant and wave functions to be isotropic, though it is required in the PL model[38–41] for amorphous semiconductors. We employ the same porous-cluster model as the previous one,[34] which has 151 Si atoms distributed on a lattice of 200 sites (see Fig. 8 in Ref. 34), because several porous clusters with different occupations (from 267 to 350 Si atoms on 450 sites) have shown similar statistical effects, i.e., the PL lifetime and the rate distribution in the absence of hopping are independent from emission energy.[46] These effects are further related to dimensional disorder of the localized wave functions as discussed in Sec. IV D.

We briefly introduce carrier kinetics for later convenience. The rate equations for the occupation numbers of radiative states $n_i^{(e)}$ for electrons in upper levels are given as[34,47,48]

$$dn_i^{(e)}/dt = \sum_j \kappa_{ij}(1-n_i^{(e)})n_j^{(e)} - \sum_j \kappa_{ji}(1-n_j^{(e)})n_i^{(e)} + \sum_j \kappa'_{ij}(1-n_i^{(e)})n_j^{(d)} - \sum_j \kappa'_{ji}(1-n_j^{(d)})n_i^{(e)} - \sum_j \alpha_{ij} n_i^{(e)} n_j^{(h)} + J_i^{(e)} \quad (3)$$

where $n_i^{(h)}$ is the occupation number for holes in lower levels and $n_i^{(d)}$ for electrons in midgap levels (nonradiative centers). On the right-hand side of Eq. (3), the first line is the flow due to hopping with the rate κ_{ij}, the second line is that due to capture by the nonradiative center with the rate κ'_{ij}, and the last line is that due to radiative recombination with the rate α_{ij}. The last term is the electron flow $J_i^{(e)}$ when an optical excitation is time independent. It is easy to obtain the rate equations for $n_i^{(h)}$ and $n_i^{(d)}$. The transition rates are given by

$$\alpha_{ij} = \alpha S_{ij}, \quad \kappa_{ij} = \kappa' S_{ij}, \quad \kappa_{ij} = \kappa S_{ij} , \quad (4)$$

where S_{ij} is the mutual overlap between wave functions of eigenstates; α is the electron-photon coupling; κ' and κ are electron-phonon couplings.[49] We write S_{ij} as

$$S_{ij} = \sum_k P_k^{(i)} P_k^{(j)} , \quad (5)$$

where $P_k^{(n)}$ represents the amplitude of nth eigenstate on the kth Si atom, i.e.,

$$P_k^{(n)} = \sum_{A=s,x,y,z} |C_{k,A}^{(n)}|^2 + \sum_{m \in k} |C_{H,m}^{(n)}|^2 . \quad (6)$$

In Eq. (6), $C_{k,A}^{(n)}$ is the component of the A-type orbital of the nth eigenstates on the kth Si atom and $C_{H,m}^{(n)}$ is that on the mth hydrogen atomic orbital. The second term on the right-hand side of Eq. (6) is the sum of the amplitudes of the wave functions over H atoms bonded to the kth Si atom, i.e., the amplitude on H atoms is assigned to a Si atom bonded to it.

The radiation intensity at an emission energy E is given by

$$I(E,t) = \sum_i \sum_j \alpha_{ij} n_i^{(e)} n_j^{(h)} \delta(E - (E_j - E_i)) , \quad (7)$$

where E_i is the energy of the ith eigenstate. After evaluating S_{ij} by a tight-binding-model calculation, the rate equations for $n_i^{(e)}$, $n_i^{(h)}$, and $n_i^{(d)}$ are solved for a given parameter γ $(=\kappa/\kappa')$, under the condition of $dn_i^{(e)}/dt = 0$ and $J_i^{(e)} \neq 0$ in the time-independent case, or under $J_i^{(e)} = 0$ in the time-dependent case. Then, the PL spectrum $I(E)$ or the decay $I(E,t)$ are calculated using Eq. (7).

B. PL properties under dominant nonradiative processes

In the case that nonradiative processes dominate ($\kappa' > \alpha$), the spectrum $I(E)$ is calculated as shown in Fig. 7. For $\gamma \leq 10^{-2}$ we see no appreciable change compared to that in the absence of hopping $\gamma = 0$. For $\gamma > 10^{-2}$, the spectrum peak shifts with γ to the low-energy side and the spectrum width narrows (see inset to Fig. 7).

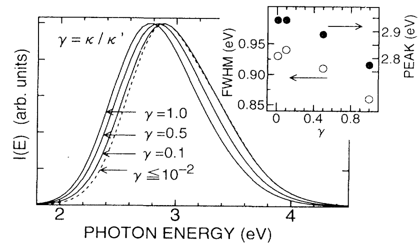

FIG. 7. Emission spectra $[I(E)$ vs $E]$ obtained for different values of γ $(=\kappa/\kappa')$ in the porous-cluster model. The inset shows the peak (●) and full width at half maximum (FWHM) (○) of the spectra plotted vs γ.

This can be understood by the flow of electrons (holes) through hopping mainly to lower (higher) energy levels when $\gamma > 10^{-2}$, which reduces the emission energies and therefore induces the spectrum redshift. Furthermore, the spectrum redshift narrows the spectrum width since the lower bound of the emission energy is limited by the energy gap of the porous cluster. When the transitions through hopping within the band are thermally activated more easily than those to nonradiative paths, i.e., for γ increasing with temperature, these spectrum redshift and narrowing agree qualitatively with experiment (Fig. 1).

The decay $I(E,t)$ at several values of E for $\gamma=0.001$, 0.01, and 0.1 has been calculated and is fitted with a stretched exponential similar to a previous study.[34] The resulting fit parameters $\kappa'\tau$ and β are shown in Fig. 8 together with ones already obtained for $\gamma=0$, 0.5 and 1.[34] For $\gamma \leq 10^{-2}$, $\kappa'\tau$ is mostly unchanged with E because the distribution of the nonradiative rates κ'_{ij} is almost independent of E (this is a statistical effect). Furthermore, since α is negligible, the bimolecular terms in Eq. (3), $\sum_j \alpha_{ij} n_i^{(e)} n_j^{(h)}$, can be omitted as second-order ones, making Eq. (3) linear. As seen later in Sec. IV C, these terms lead the decay profile to be different from a stretched exponential if radiative processes dominate. When the hopping is sizable ($\gamma > 10^{-2}$), $\kappa'\tau$ decreases exponentially with E and the decrease is steeper for larger γ as in Fig. 8(a). This is because the flow of electrons (holes) to lower (higher) levels by hopping rapidly reduces the population of electron-hole pairs which emit at higher energy, while sustaining the population of those which emit at lower energy (this is a dynamical effect). Eventually, $\kappa'\tau$ is smaller for larger E and, at large E, it is smaller for larger γ. Since κ' increases with increasing temperature, τ is smaller for higher temperature, i.e., for larger γ. Then, the results in Fig. 8 mean the plot of τ against E for larger γ (higher temperature) should be below that for smaller γ (lower temperature) similar to the observed results (Fig. 4). Meanwhile, according to Fig. 8(b), the distribution parameter β for $\gamma \leq 10^{-2}$ is small and almost independent of E. An increase in γ makes β larger for smaller E; thus β becomes a decreasing function of E, changing more steeply for larger γ. A large β at small E means that carrier hopping reduces more efficiently the variety of the decay rates contributing to PL at small E. As γ increases with temperature, these results for β are analogous to experiment (Fig. 6).

Let us assume the couplings κ and κ' are given by $\kappa=\kappa_0\exp(-W/kT)$ and $\kappa'=\kappa'_0\exp(-W'/kT)$, respectively.[47,48] Here kT is thermal energy, κ_0 and κ'_0 are constants independent of temperature T, and W and W' are activation energies. Then $\ln\tau$ is proportional to $-\ln\kappa'$ and hence to W'/T at sufficiently low temperatures, where $\gamma \ll 10^{-2}$. If this relation is applied to $T \leq 50$ K, the observed values of τ at 20 and 50 K, i.e., about 2 and 0.1 msec, respectively, give an estimate of W' to be about 10 meV; this yields the slope of the dashed line in Fig. 5. Since γ is proportional to $\exp\{-(W-W')/kT\}$, this value of W' gives a rough estimate of W to be $\sim$20 meV, if γ changes by a factor 10^2 for a change in T from 20 to 293 K.

C. PL decay under dominant radiative processes

For the electron-hole pair decaying unimolecularly, the PL intensity increases in parallel with the PL lifetime as nonradiative processes are suppressed, provided that radiative processes are negligible.[24,25] However, for temperature decrease below $\sim$70 K, the PL intensity Q slightly decreases (Fig. 1) while the PL lifetime continuously increases (Fig. 4). This observation has been ascribed to the onset of Auger effects[22] or to the dominance of radiative recombination.[5,6,24] The latter case in the present model is examined by assuming $\kappa=\kappa'=0$ and $\alpha\neq0$. The decay $I(E,t)$ and curves fit to a stretched exponential by heavily weighting the initial decay data are given in Fig. 9 for different values of E. We see that

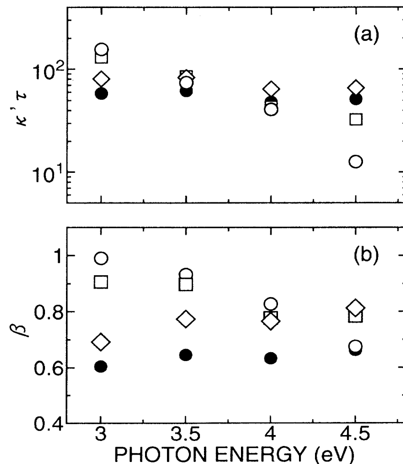

FIG. 8. Stretched-exponential parameters (a) $\kappa'\tau$ and (b) β plotted against emission energy for the decay $I(E,t)$ calculated for various γ using the porous-cluster model: $\gamma \leq 10^{-2}$ (●), and $\gamma=0.1$ (◇), 0.5 (□), and 1.0 (○).

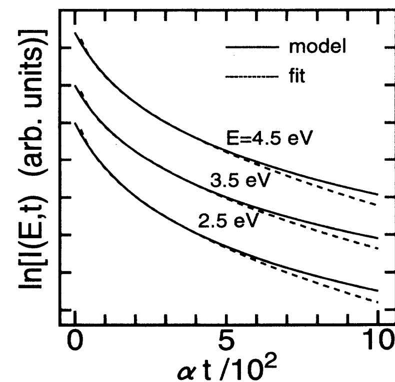

FIG. 9. The decay $I(E,t)$ (solid curve) calculated using the porous-cluster model, and the stretched-exponential fit (dashed curve) obtained under $\sigma\neq0$, $\kappa=\kappa'=0$; i.e., under the dominance of radiative processes. Note $I(E,t)$ is indepenent of E (its value is noted on each curve) and deviates from the fit in the long time regime.

$I(E,t)$ at large t increasingly deviates from the fit, because nonlinear terms $\sum_j \alpha_{ij} n_i^{(e)} n_j^{(h)}$ in Eq. (3) now dominate. These terms thus give a possible reason for the observed PL decay located above the fit at large t at 20 K (bottom of Fig. 3). Also of importance is that $I(E,t)$ is almost independent of E, suggesting the distribution of α_{ij} is independent of E; this is another statistical effect.

To explain the variation of τ with temperature, α_{ij} is presumed to be temperature dependent by including a thermal-activation factor to α, i.e., $\alpha=\alpha_0 \exp[-W^+/kT]$, where α_0 is a constant and W^+ is an activation energy. It is clear that this equation explains the observed dependence of τ on T at low temperature as the equation $\kappa'=\kappa_0 \exp(-W'/kT)$ does in the case of dominant κ'. On the other hand, the recombination rate α^* for confined excitons distributed in singlet and triplet states[5,6] is written as[50,51]

$$\alpha^* = \frac{\alpha_T + g\alpha_S \exp[-\Delta/kT]}{1+g\exp[-\Delta/kT]} , \tag{8}$$

where α_T and α_S are the recombination rates via triplet and singlet states, respectively. Here, g is a factor due to degeneracy and Δ is the splitting energy between singlet and triplet states. Although Eq. (8) represents quite different issues, it yields for small T the dependence of τ on T similar to that for α, κ, or κ' because the denominator in Eq. (8) is approximately unity for small T and $g^{-1}=3$. The observed dependence of τ on T thus merely gives an estimate of about 10 meV (compare with dashed line in Fig. 5) for the value of either W', W^+, or Δ, making it difficult to determine recombination mechanisms at low temperature.

D. Low-dimensionality in the porous-cluster model

We discuss the low-dimensional electronic wave functions for the porous-cluster model and propose their irregularity as the origin of the statistical effects. As known in percolation problems,[52] the porous cluster has the Euclidean dimensions of a perfect lattice if its concentration p is higher than a critical value, i.e., the percolation threshold p_c. Here, p denotes the number of Si-occupied sites divided by the total number of sites. The dimensions of the present porous cluster are thus 2, since $p=0.75$ while $p_c=0.7$. Wave functions in the present porous cluster, however, have *fractal* dimensions lower than 2 as shown below. This situation is quite analogous to that for wave functions in the Anderson localization problem.[53,54] In this sense, the porous cluster provides a low-dimensional electronic structure different from that in pillar or ball-like nanocrystals[1-7] in which regular crystalline structures are assumed. Meanwhile, according to the observation of two distinct pore sizes,[12] the physical porous silicon structure is not likely to be a fractal one which would show a broad distribution in pore sizes.[55,56] As shown below, electronic structures having fractal nature appropriately describe the PL characteristics of porous silicon at low temperature.

We impose the cyclic boundary conditions on the present porous cluster to yield an extended porous cluster which enables the density correlation analysis given below. Note that the extended porous cluster never yields qualitatively different characteristics from those discussed above; e.g., the PL decay for the extended porous cluster evaluated from $\kappa' > \alpha$ is well described by a stretched exponential and little affected by E $(=E_i - E_j)$ if hopping is neglected. For the porous cluster embedded in the Euclidean dimension d, we can define a fractal dimension D using the density correlation $A(L)$ given by[57]

$$A(L) = \int_0^\infty (dr_0)^d \rho(r_0) \int_0^L (dr)^d \rho(r_0+r) = cL^D , \tag{9}$$

where r_0 is a reference position, $\rho(r)$ is the density at a position r, and c is a constant of a length scale L. By plotting $\ln A(L)$ against $\ln(2L+1)$, we can examine whether or not Eq. (9) holds, and if it holds we can determine D. Here, $(2L+1)^d$ is the volume for the portion of the extended porous cluster, i.e., the number of unit cells in it. (The present unit cell is that of a honeycomb lattice and contains two sites.) It is revealed that D is equal to 2 if the atomic density is taken for $\rho(r)$, while if $\rho(r)$ is replaced by the electron (hole) density defined by $P_k^{(n)}$ in Eq. (6), D is less than 2, implying the eigenfunction of the electron (hole) to be fractal. The examples of such plots for electron density are shown in Fig. 10 where $\ln A(L)$ shows a linear dependence on $\ln(2L+1)$ with a slope less than 2. The values of D for various eigenenergies E_i are shown in Fig. 11. It can be seen that D is uncorrelated to E_i, and therefore, to emission energy E. Even for an emission at a single E, a variety of wave functions having different D clearly contributes, implying dimensional disorder, yielding a broad distribution of decay rates or a stretched-exponential PL decay. The independence of D

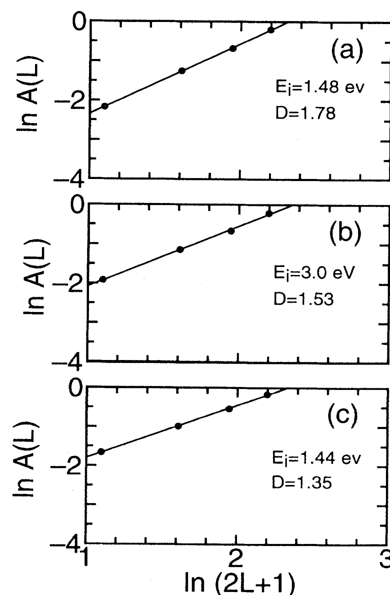

FIG. 10. The electron-density correlation $\ln A(L)$ vs $\ln(2L+1)$: the linear slope of this plot determines the fractal dimension D of the wave function with eigenenrgy E_i.

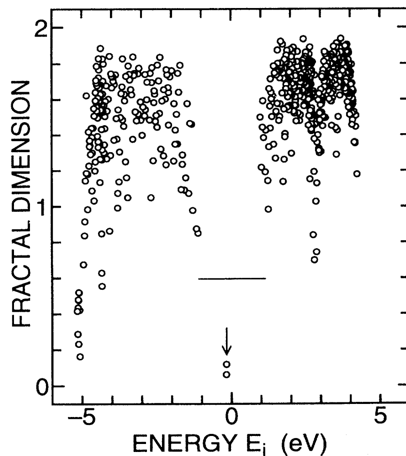

FIG. 11. Fractal dimension D of the wave function in the porous-cluster model plotted against its eigenenergy E_i.

from E is a statistical effect of the model.

Insofar as surface-related processes dominate,[8–10] the two-dimensional porous cluster is not unrealistic, since it qualitatively describes well the PL properties of porous silicon. We consider, however, that dimensional disorder in the model rather than Euclidean dimensions plays a role in the PL characteristics. Preliminary results[46] on a three-dimensional but small porous cluster with 270 atoms in six layers at $p=0.43$ show that the PL decay still behaves similarly to that in this study; e.g., the PL decay without hopping of carriers is mostly independent of emission energy and its profile is described by a stretched exponential. Although atoms in the porous cluster are presumed to maintain their lattice positions in the above discussion, configurational relaxation of atoms may occur after producing the porous cluster. If the relaxation does not alter the coordination numbers for individual atoms, this simplification might not seriously change the qualitative results above. In this sense, a special lattice structure might be of secondary importance compared to the topological connectivities of the atoms. These, however, are problems left for the future.

V. CONCLUSION

PL of porous silicon is studied at various temperatures (15–293 K) and its properties are interpreted using a porous-cluster model. Below ~70 K, the nonexponential PL decay is mostly independent of emission energy $E_{\rm PL}$. This is ascribed to the carrier recombination through localized states distributed in energies, which give a distribution of wave-function overlap independent of emission energy (statistical effects). Further, the low dimensionality in terms of a fractal dimension of wave function and its disorder in the electronic structure of the porous cluster model are put forward for the origin of the statistical effects. As the temperature increases, on the other hand, the PL spectrum redshifts, the spectrum width narrows, and the PL lifetime decreases. The PL lifetime becomes a decreasing function of $E_{\rm PL}$. These changes by temperature are conceived to be induced by thermal activation of recombination processes, including carrier hopping among these localized states (dynamical effects).

ACKNOWLEDGMENTS

We thank Dr. N. Hamada, Dr. Y. Mochizuki, Professor H. Sumi (Tsukuba University) and Professor H. Kamimura (Tokyo Science Univ.) for fruitful discussion. Thanks are also due to Dr. R. Lang and Dr. N. Shohata for their support, and to Dr. D. J. Tweet for his reading of this manuscript.

[1] L. T. Canham, Appl. Phys. Lett. **57**, 1046 (1990).
[2] A. G. Cullis and L. T. Canham, Nature **353**, 335 (1991).
[3] V. Lehmann and U. Gösele, Appl. Phys. Lett. **58**, 856 (1991).
[4] T. Suemoto, K. Tanaka, A. Nakajima, and T. Itakura, Phys. Rev. Lett. **70**, 365 (1993).
[5] P. D. J. Calcott, K. J. Nash, L. T. Canham, M. J. Kane, and D. Brumhead, J. Lumin. **57**, 257 (1993).
[6] P. D. J. Calcott, K. J. Nash, L. T. Canham, M. J. Kane, and D. Brumhead, J. Phys. Condens. Matter **5**, L91 (1993).
[7] S. Schuppler, S. L. Friedman, M. A. Marcus, D. L. Adler, Y.-H. Xie, F. M. Ross, T. Harris, W. L. Brown, Y. J. Chabal, L. E. Brus, and P. H. Citrin, Phys. Rev. Lett. **72**, 2648 (1994).
[8] F. Koch, V. P-Koch, T. Muschik, A. Nikolov, and V. Gabrilenko, in *Microcrystalline Semiconductors: Materials Science and Devices,* edited by P. M. Fauchet, C. C. Tsai, L. T. Canham, I. Shimizu, and Y. Aayagi, MRS Symposia Proceedings No. 283 (Materials Research Society, Pittsburgh, 1993), p. 197.
[9] F. Koch, V. P-Koch, and T. Muschik, J. Lumin. **57**, 271 (1993).
[10] Y. Kanemitsu, Phys. Rev. B **48**, 12 357 (1993).
[11] J. Zeman, M. Zigone, G. Martinez, and G. L. J. A. Rikken, Europhys. Lett. **26**, 625 (1994).
[12] V. Lehmann, J. Electrochem. Soc. **140**, 2836 (1993).
[13] N. Noguchi, I. Suemune, M. Yamanishi, G. C. Hua, and N. Otsuka, Jpn. J. Appl. Phys. **31**, L490 (1992).
[14] T. George, M. S. Anderson, W. T. Pike, T. L. Lin, R. W. Fathauer, K. H. Jung, and D. L. Kwong, Appl. Phys. Lett. **60**, 2359 (1992).
[15] R. P. Vasquez, R. W. Fathauer, T. George, A. Ksendzov, and T. L. Lin, Appl. Phys. Lett. **60**, 1004 (1992).
[16] C. Tsai, K.-H. Li, D. S. Kinosky, R.-Z. Qian, T.-C. Hsu, J. T. Irby, S. K. Banerjee, A. F. Tasch, J. C. Campbell, B. K. Hance, and J. White, Appl. Phys. Lett. **60**, 1700 (1992).
[17] V. P-Koch, T. Muschik, A. Kux, B. K. Meyer, and F. Koch, Appl. Phys. Lett. **61**, 943 (1992).
[18] M. S. Brandt, H. D. Fuchs, M. Stutzmann, J. Weber, and M.

Cardona, Solid State Commun. **81**, 307 (1992).

[19]P. Deak, M. Rosenbauer, M. Stutzmann, J. Weber, and M. Brandt, Phys. Rev. Lett. **69**, 2531 (1992).

[20]S. L. Friedman, M. A. Marcus, D. L. Adler, Y.-H. Xie, T. D. Harris, and P. H. Citrin, Appl. Phys. Lett. **62**, 1934 (1993).

[21]X. L. Zheng, W. Wang, and H. C. Chen, Appl. Phys. Lett. **60**, 986 (1992).

[22]Y. Mochizuki, M. Mizuta, Y. Ochiai, S. Matsui, and N. Ookubo, Phys. Rev. B **46**, 12 353 (1992).

[23]Z. Y. Xu, M. Gal, and M. Gross, Appl. Phys. Lett. **60**, 1375 (1992).

[24]W. L. Wilson, P. F. Szajowski, and L. E. Brus, Science **262**, 1242 (1993).

[25]J. C. Vial, A. Bsiesy, F. Gaspard, R. Herino, M. Ligeon, F. Muller, R. Romestain, and R. M. Macfarlane, Phys. Rev. B **45**, 14 171 (1992).

[26]T. Matsumoto, H. Mimura, and Y. Kanemitsu, J. Phys. Soc. Jpn. Suppl. B **63**, 182 (1994).

[27]A. Bsiesy, J. C. Vial, F. Gaspard, R. Henrino, M. Ligeon, F. Muller, R. Romestain, A. Wasiela, A. Haliamaoui, and G. Bomchil, Surf. Sci. **254**, 195 (1991).

[28]M. A. Tishler, R. T. Collis, J. H. Stathis, and J. C. Tsang, Appl. Phys. Lett. **60**, 639 (1992).

[29]Y. H. Xie, W. L. Wilson, F. M. Ross, J. A. Mucha, E. A. Fitzgerald, J. M. Macaulay, and T. D. Harris, J. Appl. Phys. **71**, 2403 (1992).

[30]N. Ookubo, H. Ono, Y. Ochiai, Y. Mochizuki, and S. Matsui, Appl. Phys. Lett. **61**, 940 (1992).

[31]N. Ookubo, J. Appl. Phys. **74**, 6375 (1993).

[32]L. Pavesi and M. Ceschini, Phys. Rev. B **48**, 17 625 (1993).

[33]H. Scher, M. F. Shlesinger, and J. T. Bendler, Phys. Today **44**, (1), 26 (1991).

[34]S. Sawada, N. Hamada, and N. Ookubo, Phys. Rev. B **49**, 5236 (1994).

[35]P. J. Caplan, E. H. Poindexter, B. E. Deal, and R. Razouk, J. Appl. Phys. **50**, 5847 (1979).

[36]K. L. Brower, Phys. Rev. B **33**, 4471 (1986).

[37]M. Kondo and H. Yokomichi, J. Phys. Soc. Jpn. Suppl. B **63**, 145 (1994).

[38]R. A. Street, in *Semiconductor and Semimetals,* edited by J. I. Pankove (Academic, Orlando, 1984), Vol. 21, Pt. B, Chap. 5.

[39]S. F. Edwards, J. Noncryst. Solids **4**, 417 (1970).

[40]R. A. Abram and S. F. Edwards, J. Phys. C **5**, 1183 (1972).

[41]R. A. Street, Solid State Commun. **34**, 157 (1980).

[42]Y. Chen, Phys. Rev. B **41**, 10 604 (1990).

[43]N. Ookubo, Y. Matsuda, and N. Kuroda, Appl. Phys. Lett. **63**, 346 (1993).

[44]V. Gösele and V. Lehmann, in *Extended Abstracts of the 1992 International Conference on Solid State Devices and Materials, Tsukuba, Japan,* edited by Y. Nannichi (The Japan Society of Applied Physics, Tokyo, 1992), p. 469.

[45]K. C. Pandey and J. C. Phillips, Phys. Rev. B **13**, 750 (1976).

[46]S. Sawada and N. Ookubo (unpublished).

[47]R. Engleman and J. Jortner, Mol. Phys. **18**, 145 (1970).

[48]N. Robertson and L. Friedman, Philos. Mag. **33**, 753 (1976).

[49]N. F. Mott and E. A. Davis, *Electronic Processes in Non-Crystalline Materials* (Clarendon, Oxford, 1979).

[50]J. Weber, W. Schmid, and R. Sauer, Phys. Rev. B **21**, 2401 (1980).

[51]U. Schall, K. Thonke, and R. Sauer, Phys. Status Solidi B **137**, 305 (1986).

[52]D. Stauffer, *Introduction to Percolation Theory* (Taylor & Francis, London, 1985).

[53]M. Schreiber, Physica A **167**, 188 (1990).

[54]M. Schreiber and H. Grussbach, Phys. Rev. Lett. **67**, 607 (1991).

[55]J. Harsanyi and H.-U. Habermeier, Microelectron. Eng. **6**, 575 (1987).

[56]R. L. Smith, S.-F. Chuang, and S. D. Collins, Sens. Actuators **A21-A23**, 825 (1990).

[57]C. M. Soukoulis and E. N. Economou, Phys. Rev. Lett. **52**, 565 (1984).